E.-C. Kang, A. Ogura, K. Kataoka, Y. Nagasaki	Preparation of water-soluble PEGylated semiconductor nanocrystals	Chemistry Letters	33(7)	840-841	2004
H. Hayashi, M. Iijima, K. Kataoka, Y. Nagasaki	pH-Sensitive nanogel possessing reactive PEG tethered chains on the surface	Macromolecules	37(14)	5389-5396	2004
E. Jule, Y. Yamamoto, M. Thouvenin, Y. Nagasaki, K. Kataoka	Thermal characterization of poly(ethylene glycol)-poly(D,L-lactide) block copolymer micelles based on pyrene excimer formation	J. Controlled Release	97(3)	407-419	2004
Y. Kakizawa, S. Furukawa, K. Kataoka	Block copolymer-coated calcium-phosphate nanoparticles sensing intracellular environment for oligodeoxynucleotide and siRNA delivery	J. Controlled Release	97(2)	345-356	2004
A. Matsumoto, R. Yoshida, K. Kataoka	Glucose-responsive polymer gel bearing phenylborate derivative as a glucose-sensing moiety operating at the physiological pH	Biomacromolecules	5(3)	1038-1045	2004
Y. Kakizawa, K. Miyata, S. Furukawa, K. Kataoka	Size-controlled formation of a calcium phosphate-based organic-inorganic hybrid vector for gene delivery using poly(ethylene glycol)-block-poly(aspartic acid)	Advanced Materials	16(8)	699-702	2004
H. Otsuka, A. Hirano, Y. Nagasaki, T. Okano, Y. Horiike, K. Kataoka	Two-dimensional multiarray formation of hepatocyte spheroids on a microfabricated PEG-brush surface	ChemBioChem	5(6)	850-855	2004
H. Katakura, A. Harada, K. Kataoka, M. Furusho, F.	Improvement of retroviral vectors by coating with poly(ethylene	J. Gene Medicine	6(4)	471-477	2004

Tanaka, H. Wada, K. Ikenaka	glycol)-poly(L-lysine) block copolymer (PEG-PLL)				
D. Wakebayashi, N. Nishiyama, Y. Yamasaki, K. Itaka, N. Kanayama, A. Harada, Y. Nagasaki, K. Kataoka	Lactose-installed polyion complex micelles incorporating plasmid DNA as a targetable gene vector system: Their preparation and gene transfecting efficiency against cultured HepG2 cells	J. Controlled Release	95(3)	653-664	2004
Y. Akiyama, Y. Nagasaki, K. Kataoka	Synthesis of heterotelechelic poly(ethylene glycol) derivatives having a-benzaldehyde and w-pyridyl disulfide groups by ring opening polymerization of ethylene oxide using 4-(diethoxymethyl)benzyl alkoxide as a novel initiator	Bioconjugate Chemistry	15(2)	424-427	2004
M. Jaturanpinyo, A. Harada, X. Yuan, K. Kataoka	Preparation of bionanoreactor based on core-shell structured polyion complex micelles entrapping trypsin in the core cross-linked with glutaraldehyde	Bioconjugate Chemistry	15(2)	344-348	2004
K. Miyata, Y. Kakizawa, N. Nishiyama, A. Harada, Y. Yamasaki, H. Koyama, K. Kataoka	Block catiomer polyplexes with regulated densities of charge and disulfide cross-linking directed to enhance gene expression	J. Amer. Chem. Soc.	126(8)	2355-2361	2004
M. Tabuchi, M. Ueda, N. Kaji, Y. Yamasaki, Y. Nagasaki, K. Yoshikawa, K. Kataoka, Y. Baba	Nano-spheres for DNA separation chips	Nature Biotechnology	22(3)	337-340	2004
C. Diab, Y. Akiyama, K. Kataoka, F. M. Winnik	Microcalorimetric Study of the Temperature-Induced Phase	Macromolecules	37(7)	2556-2562	2004

	Separation in Aqueous Solutions of Poly(2-isopropyl-2-oxazolines)				
A. Matsumoto, T. Kurata, D. Shiino, K. Kataoka	Swelling and shrinking kinetics of totally synthetic, glucose-responsive polymer gel bearing phenylborate derivative as a glucose-sensing moiety	Macromolecules	37(4)	1502-1510	2004
R. Ideta, Y. Yanagi, Y. Tamaki, F. Tasaka, A. Harada, K. Kataoka	Effective accumulation of polyion complex micelle to experimental choroidal neovascularization in rats	FEBS Lett.	557(1-3)	21-25	2004
T. Kajiyama, H. Kobayashi, K. Morisaku, T. Taguchi, K. Kataoka, J. Tanaka	Determination of end-group structures and by-products of synthesis of poly(□,□-malic acid) by direct polycondensation	Polymer Degradation and Stability	84(1)	151-157	2004

NANO LETTERS

2004
Vol. 4, No. 11
2163−2169

Physicochemical Properties and Cellular Toxicity of Nanocrystal Quantum Dots Depend on Their Surface Modification

Akiyoshi Hoshino,[†,‡,§] Kouki Fujioka,[†] Taisuke Oku,[†] Masakazu Suga,[†] Yu F. Sasaki,[∥] Toshihiro Ohta,[⊥] Masato Yasuhara,[‡] Kazuo Suzuki,[§] and Kenji Yamamoto*[,†,‡]

Department of Medical Ecology and Informatics, Research Institute, International Medical Center of Japan, Toyama 1-21-1, Shinjuku, Tokyo 162-8655, Japan, Department of Pharmacokinetics and Pharmacodynamics, Hospital Pharmacy, Tokyo Medical and Dental University Graduate School, Yushima 1-5-45, Bunkyo-ku, Tokyo 113-8519, Japan, Department of Bioactive Molecules, National Institute of Infectious Diseases, Toyama 1-23-1, Shinjuku, Tokyo 162-8640, Japan, Faculty of Chemical and Biological Engineering, Hachinohe National College of Technology, Tamonoki Uwanotai 16-1, Hachinohe, Aomori 039-1192, Japan, and School of Life Science, Tokyo University of Pharmacy and Life Science, Horinouchi 1432-1, Hachioji, Tokyo 192-0392, Japan

Received August 9, 2004; Revised Manuscript Received October 5, 2004

ABSTRACT

Nanocrystal quantum dots (QDs) have been applied to molecular biology because of their greater and longer fluorescence. Here we report the potential cytotoxicity of our characterized QDs modified with various molecules. Surface modification of QDs changed their physicochemical properties. In addition, the cytotoxicity of QDs was dependent on their surface molecules. These results suggested that the properties of QDs are not related to those of QD-core materials but to molecules covering the surface of QDs.

The behavior of QDs in biological systems is not dependent on the chemical properties of surface-covered molecules but on the nanocrystal particle itself. The surface treatment of nanocrystals (surface-covered functional groups and biomolecules covering the surface of QDs) has specified the biological behavior of whole nanocrystal QDs.

With the development of nanotechnology engineering, nanomaterial products such as carbon nanotubes, fullerenes, and nanocrystal quantum dots (QDs) are now widely produced and consumed. Great quantities of those "artificial nanomaterials" have been used on the premise of being biologically and environmentally harmless, although only a few studies have reported the cellular toxicity of those materials.[1] These artificial nanomaterials are so small that they may be easily spread, stored in the environment and even in our body, and disrupt some functions of living organism consisting of complicated natural nanomaterials. It cannot be denied that these artificial nanomaterials are also detrimental, once small substances such as asbestos, coarse particulates, and particle matter exhaust from diesel engines proved to be harmful.[2−4] Thus, we need to investigate the potential toxicity of artificial nanomaterials.

QDs are now becoming widely used in biotechnology and medical applications.[5−12] QDs have several advantages over organic fluorophores with regard to high luminescence, stability against photobleaching, and a range of fluorescence wavelengths from blue to infrared depending on the particle size.[13] However, QDs aggregate easily and lose luminescence in an intracellular environment, even under acidic (pH < 5) or isotonic conditions. Therefore, it was considered difficult to replace conventional organic fluorescent probes completely with QDs.[14] Recently, some improvements were reported to prevent aggregation under intracellular conditions by the conjugation of biomolecules with QDs,[15−18] and some are used in immunohistochemical staining.[17−19] In this study, we developed several novel surface-modified QDs using carboxylic acids, polyalcohols, and amines and evaluated their physicochemical character and cytotoxicity. There are few

* Corresponding author. E-mail: backen@ri.imcj.go.jp. Tel: +81-3-3202-7181 ext 2856. Fax: +81-3-3202-7364.
† International Medical Center of Japan.
‡ Tokyo Medical and Dental University Graduate School.
§ National Institute of Infectious Diseases.
∥ Hachinohe National College of Technology.
⊥ Tokyo University of Pharmacy and Life Science.

10.1021/nl048715d CCC: $27.50
Published on Web 10/16/2004

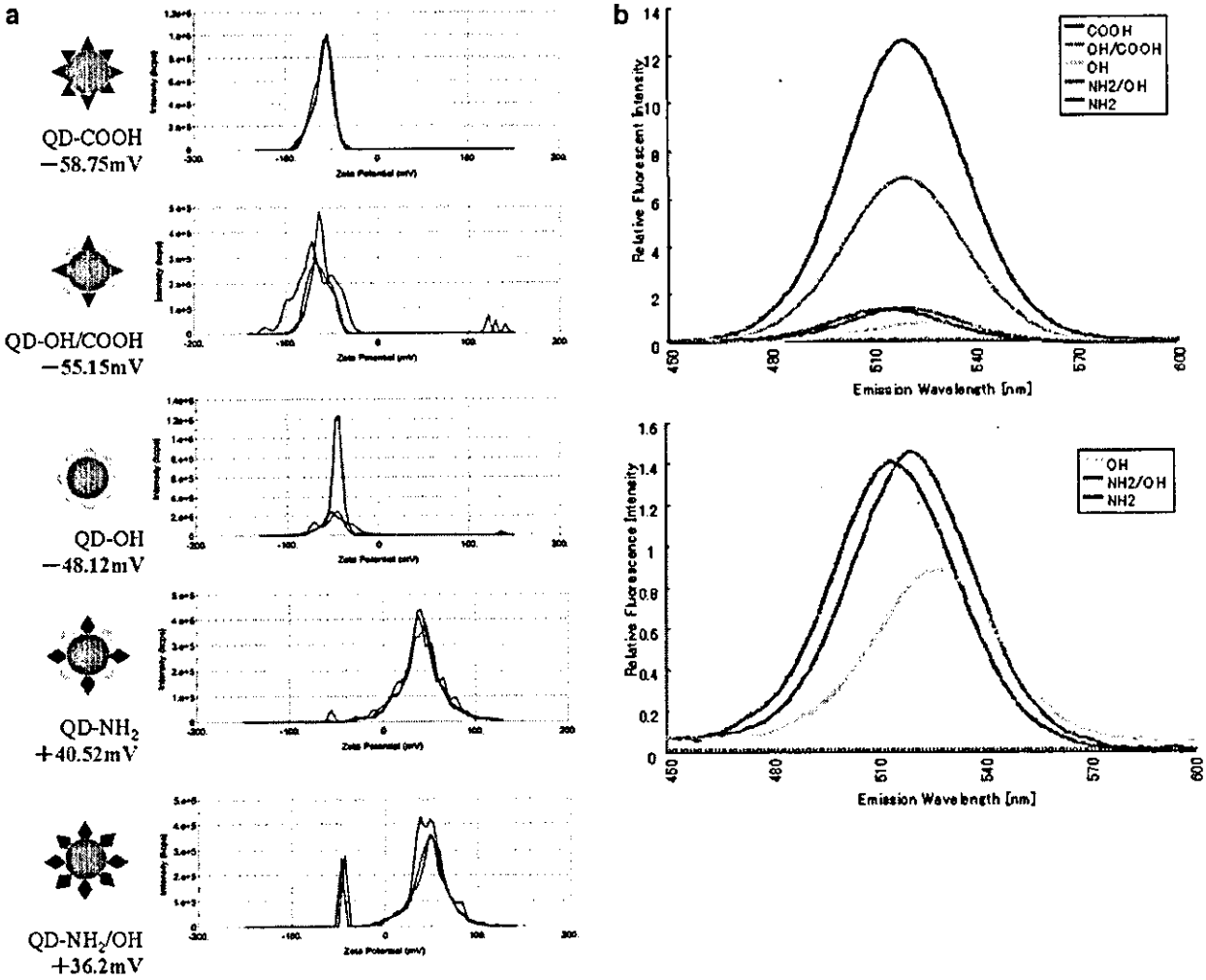

Figure 1. Surface ζ potential and fluorescence intensity of QDs varied by their surface modification. (a) Cartoon (left) and ζ potential (right) of the novel modified QDs. Surface zeta-potential of QDs is measured by electrophoresis. Each line shows the electrophoretic mobility of QDs in the stationaly layers. The data are the average of 30 assays. (b) Relative fluorescence intensity and peak wavelength of QDs measured by fluorescence spectrometry. (Lower) enlarged panel of QD-OH (yellow); QD-NH_2/OH (green) and QD-NH_2 (blue) in the upper panel. The peak emission wavelengths of QD-COOH, QD-OH/COOH, QD-OH, QD-NH_2/OH, and QD-NH_2 varied at 519, 520, 526, 520, and 513 nm, respectively.

studies on the cytotoxicity of QDs in mammalian cells, although several experiments applying to living cells and animals have already been performed.[19−25] In this study, we tested the cytotoxic potential of QDs by three different assays: comet assay, flow cytometry, and MTT assay. The comet assay, which detects DNA damage by gel electrophoresis, has been widely used to detect apoptotic cell damage induced by chemicals.[26−29] In this assay, DNA fragments can be observed as a stream from the nucleus, and the level of damage can be quantitated by the length of the stream of DNA fragments. We report here that the cytotoxicity of QDs is also caused by the surface-covering molecules of QDs but not by the nanocrystalline particle itself.

We synthesized ZnS-coated CdSe nanocrystal QDs (518-nm fluorescence peak emission). Synthesized QDs were then coated with MUA (QD-COOH), cysteamine (QD-NH_2), or thioglycerol (QD-OH) using thiol-exchange reactions as previously described.[30−32] To introduce two functional groups (QD-OH/COOH, and QD-NH_2/OH), we used equal molar quantities of thioglycerol and MUA or cysteamine and thioglycerol, respectively. To investigate the physicochemical properties of these five types of modified QDs, we measured the fluorescence intensity, particle diameter, and surface ζ potential. At first, we assessed the surface ζ potential of QDs to confirm whether the exchange reaction was performed (Figure 1a). As expected, QD-COOH and QD-OH/COOH were highly negatively charged, whereas QD-NH_2 and QD-NH_2/OH were positively charged. QD-OH was less negatively charged than the carboxylic acid groups. QDs with both hydroxyl and carboxyl/amine groups had median charge in both groups. We then assessed whether the difference in the surface modification of QDs affected the fluorescence intensity. The fluorescence intensity and peak wavelength

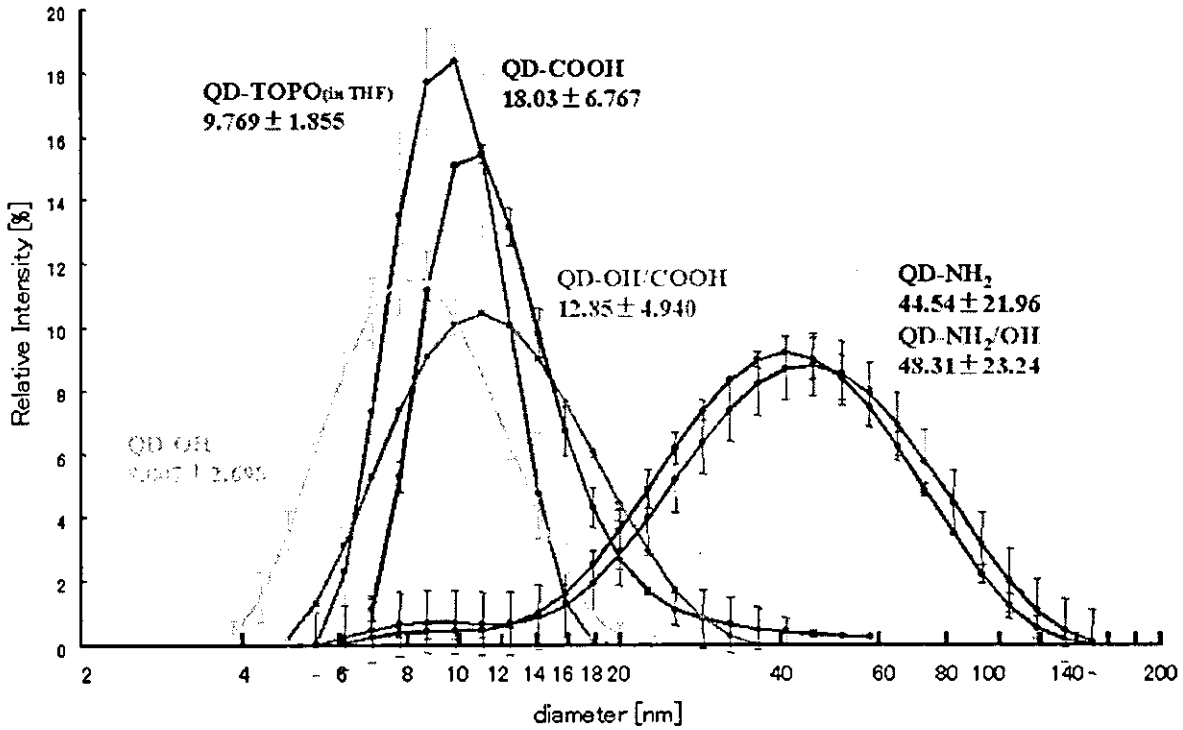

Figure 2. Size distribution of modified QDs in aqueous solution varied by their surface modification. The profile for the distribution of QDs in aqueous solution was observed by dynamic light scattering methods. Values are the mean ± standard deviation of the data measured 12 times, respectively.

were measured using a fluorescence spectrometer (Figure 1b). The QDs of carboxyl groups had higher luminescence than the other groups. Furthermore, the peak wavelength varied according to the surface modification. QDs containing amino groups emitted a shorter wavelength than the originally synthesized QD (TOPO capped-QD; 518-nm emission). In contrast, QDs with hydroxyl groups were slightly red-shifted. We assumed that a longer carbon chain and the carboxyl groups of MUA may contribute to the long lifetime and high quantum yield of QD-COOH. In contrast, the decreasing fluorescence of amino-QD particles may be caused by the oxidation of QD-metal because of the leakage of electrons from QDs through NH_2 groups in aqueous solution.[13] This suggested that the luminescence intensity of QDs may increase according to the surface-covered molecule structures.

Although it is known that the fluorescence of QDs depends on the particle size, the interparticle conformation of QDs in aqueous solution has not yet been revealed. To investigate whether any change in the particle conformation of QDs occurred in the process of surface modification, we attempted to measure the particle diameter of QDs by dynamic light scattering (DLS). We used a He−Ne laser (633-nm wavelength) light source because using a short wavelength that excites the QDs impedes the detection of QD light scattering. The size distribution of QDs was widely spread according to their modifications (Figure 2). Amino-QDs showed a broad particle distribution around 40 nm. In contrast, QDs of carboxyl groups had a narrow distribution around 20 nm. These results seemed to be contradicted by the observation that the emission wavelength of QDs depended on their particle size.[11,34] In addition, it was previously reported that transmission electron microscopy showed the diameter of the uncoated green nanocrystalline QD to be approximately 3.5 nm.[31] Positively charged amino-QDs and negatively charged impure materials in solution (such as TOPO) may form an ionic combination and affect the "apparent" diameter of the particles. In the case of carboxyl QDs, hydrophobic interaction among long carbon chains is also concerned with their larger particle distribution.

Processing the QD surface with hydroxyl group resulted in improved dispersion and stability under hypertonic conditions (Figure 3). In contrast, all of the QDs were stable in nonelectrolyte solutions. All of the modified QDs were stable for 30 min under weak alkaline conditions, whereas only QDs of the amine groups were stable under acidic conditions. These results were useful for advanced surface development to apply QDs in biological and medical fields.

To examine whether QDs affected cell proliferation, we first assessed cell proliferation by MTT assay. The reduction activity of cells was decreased by adding the crude QDs (Figure 4), but we cannot determine whether the amine-QDs were harmful because MTT reagensts were nonbiologically reduced to hormazan by the amine-QDs (data not shown). Then we determined whether this damage was caused by cell death or the suppression of cell activity. To examine whether the cell damage of QDs was affected by their surface potential, the cytotoxicity was evaluated by flow

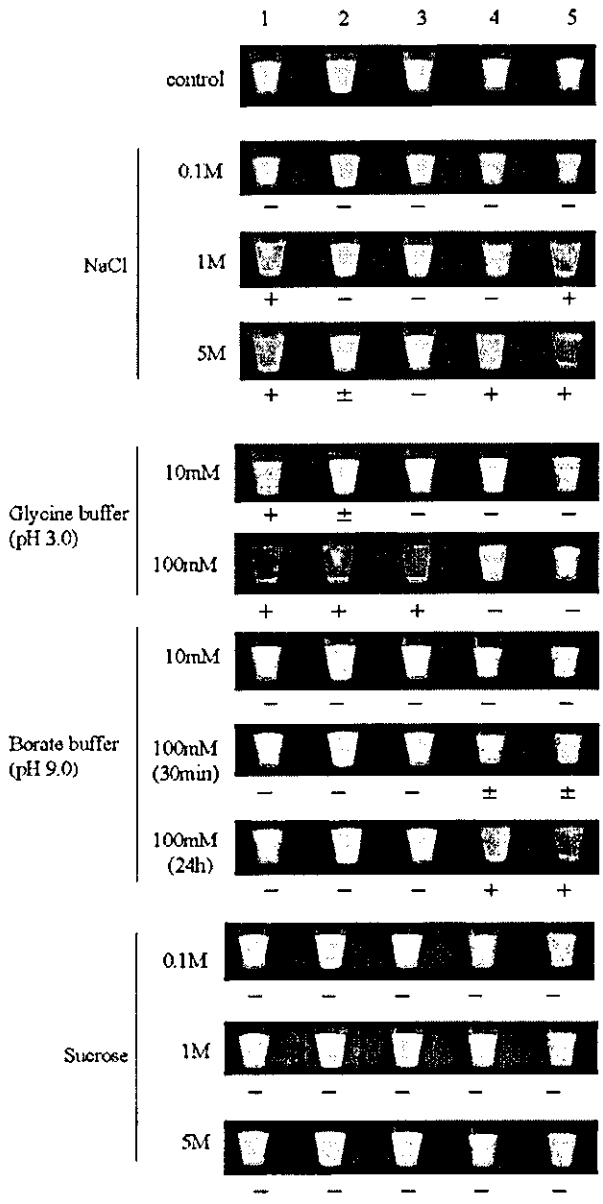

Figure 3. Physicochemical stability of various modified QDs in aqueous buffers. A QD aqueous solution (10 μM) was diluted by the indicated buffers (QD final concentration 100 nM), and incubated for 30 min at room temp. The snapshots were captured using a digital camera with $^1/_{30}$ s exposure excited by a 365-nm wavelength (UV-A). The results were reproduced in three separate experiments. 1, QD-COOH; 2, QD-OH/COOH; 3, QD-OH, 4, QD-NH_2/OH; 5, QD-NH_2; +, aggregated; ±, partially aggregated; −, not aggregated.

cytometry (Figure 5). QDs were introduced into cells by an endocytotic mechanism by adding culture media.[14,25] Cell death was observed by adding crude QDs. In contrast, low cell damage and high labeling efficiency were achieved by adding purified QDs. However, slight cell death was observed only by purified QD-COOH. This cytotoxicity may be caused by uptake QDs located in endosomes.[14] As surface molecules were bound to QDs through the electric interaction

Table 1. DNA-Damaging Effects of the Ingredients and Impurities of the QD Samples

compound	dose (μg/mL)	tail length of 50 nuclei (mm, mean ± SE) 2-h treatment	12-h treatment
MUA	0	23.4 ± 1.05	23.9 ± 1.21
	25	25.6 ± 0.58	28.1 ± 1.31
	50	33.8 ± 2.38[a]	41.2 ± 3.31[a]
	100	54.6 ± 3.27[a]	toxic
	200	76.0 ± 3.52[a]	toxic
	400	80.3 ± 3.18[a]	toxic
cysteamine	0	23.5 ± 0.81	24.1 ± 1.05
	50	22.4 ± 0.40	25.1 ± 1.12
	100	23.4 ± 0.95	29.6 ± 1.72
	200	22.9 ± 0.90	35.4 ± 2.89[a]
	400	23.3 ± 0.82	44.5 ± 2.21[a]
thioglycerol	0	23.5 ± 0.81	24.1 ± 1.05
	50	24.7 ± 1.06	27.0 ± 1.65
	100	26.0 ± 1.28	24.7 ± 1.24
	200	22.4 ± 0.83	24.6 ± 0.99
	400	23.4 ± 0.98	28.1 ± 1.84
TOPO	0	23.8 ± 0.91	23.1 ± 1.04
	50	24.9 ± 0.47	22.5 ± 0.56
	100	27.1 ± 1.33	26.3 ± 1.81
	200	29.6 ± 1.92	28.1 ± 1.33
	400	32.5 ± 1.43[a]	31.7 ± 1.31[a]
ZnS	0	23.8 ± 0.91	23.1 ± 1.04
	50	23.7 ± 0.89	24.1 ± 0.51
	100	22.5 ± 0.53	22.4 ± 0.34
	200	24.1 ± 0.71	24.1 ± 0.56
	400	23.3 ± 0.54	22.2 ± 0.97

[a] $P < 0.05$.

between the sulfhydryl group and QD-covered zinc,[25] surface molecules such as MUA may be detached by acidic and oxidative conditions in endosomes and released into cytoplasm.[34] The fluorescence of QDs was lost by low pH, by oxidation of the surface structures, or by some intracellular factors adsorbed onto QDs,[13] implying that the advanced development of the surface modification of QDs needs to overcome the cytotoxicity. However, this detachment could be utilized to release valuable materials such as medicines and genes into cells by cellular oxidative/reductive conditions.

Next, to investigate whether cell death by QDs was carried out by an apoptotic pathway, we evaluated the genotoxic potential of QDs by comet assay with WTK1 cells.[27-29] A significant increase in the tail length was observed after 2 h of treatment with QD-COOH at 2 μM (Figure 6a). After treatment for 12 h, the tail length was equal to that of the control cells, suggesting that the induced DNA damage was efficiently repaired during prolonged incubation. Crude QD-COOH samples prepared by only membrane filtration, but not by ultrafiltration, showed stronger DNA damage than purified QD-COOH (Figure 6b). However, QD-NH2, QD-OH, QD-OH/COOH, and QD-NH2/OH induced no DNA damage up to a dose of 4 μM for 2 h. To determine whether the genotoxicity of QDs was caused by QD particles themselves, three ingredients of the QD samples (MUA, cysteamine, and thioglycerol) and two possible impurities (TOPO and ZnS) were also assayed. As shown

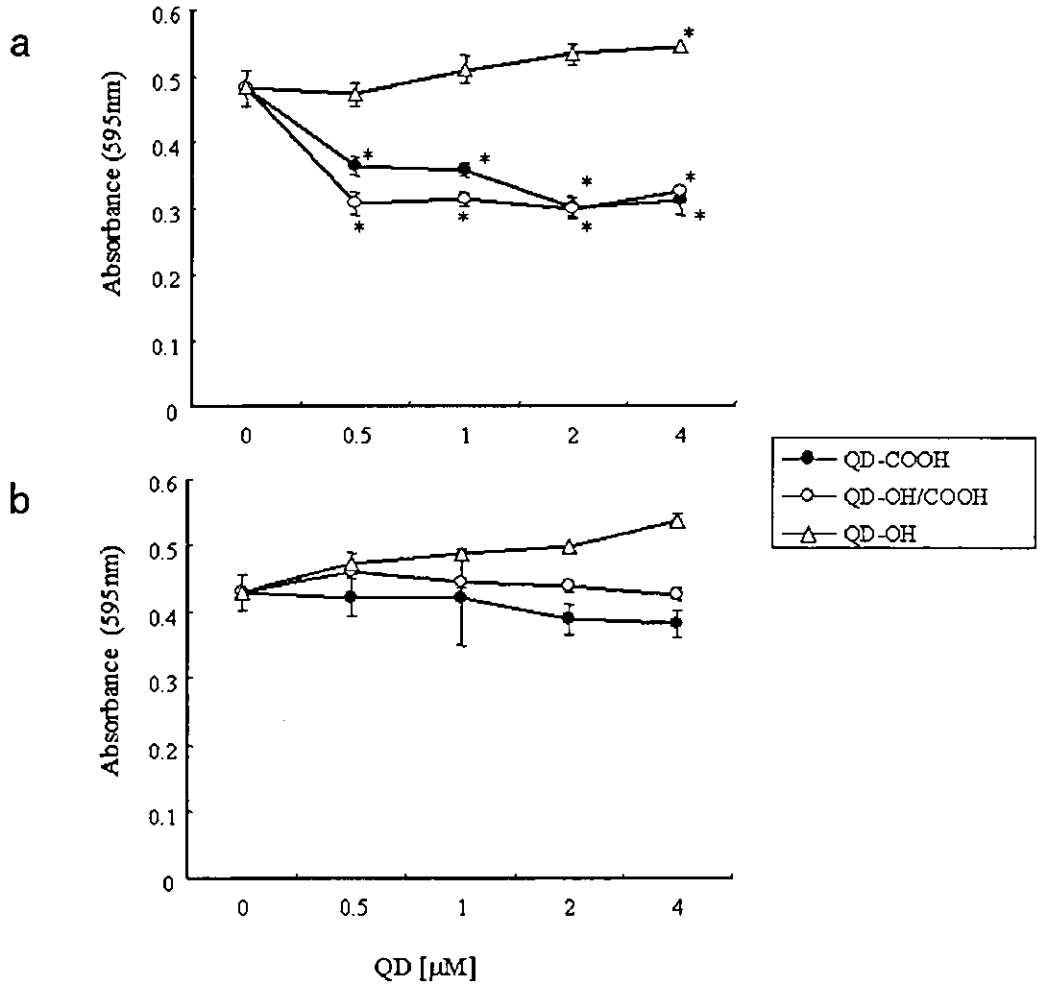

Figure 4. Contaminated impurities and ingredients in QD samples suppress the proliferation of cultured cells. Vero cells were plated at 5×10^4 cells on 96-well plates and cultured for 4 h with (a) crude QD and (b) ultrafiltartion-purified QDs in coexisting MTT reagents (Roche Diagnostics). After incubation, the cells were lysed on the plate, and 595-nm absorbance (reduced hormazan) was measured with a microplate reader. Data are presented as the mean ± standard deviation of duplicate samples. Significance was evaluated by the *t* test versus negative control. *, $p < 0.05$.

in Table 1, treatment with MUA for 12 h caused severe cytotoxicity at doses greater than 100 μg/mL (approximately coordinated to 4μM QD-COOH). DNA damage was observed at doses greater than or equal to 50 μg/mL with 2 h of treatment. Cysteamine was weakly genotoxic when cells were treated for 12 h. Thioglycerol was negative in the assay, suggesting that QD-OH was the least toxic QD among them. Because TOPO was also found to be a cytotoxic and genotoxic compound, the complete removal of TOPO from the QD samples is important in reducing toxicity. These results provided evidence that some hydrophilic compound-coated QDs are responsible for the genotoxicity of QD. Almost all of the DNA damage induced by QD-COOH was efficiently repaired in the cells because DNA damage detected by the comet assay did not persist in the cells treated for 12 h. However, the possibility remains that a few nonrepaired DNA lesions can result in gene mutations or chromosome aberrations. These results provided evidence that some hydrophilic compound-coated QDs are responsible for the cytotoxicity of QDs. It is an important factor for designing less-toxic QDs to select hydrophilic compounds to dissolve QDs in water. These results suggested that the surface treatment of nanocrystals (surface-covered functional groups and biomolecules covered the surface of QDs) has specified the biological behavior of whole nanocrystal QDs.

Nanocrystal QDs have the great potential to be applied to molecular biology and bioimaging because of several advantages over organic fluorophores. As of now, the potential toxicity of industrial products is not considered, whereas the pharmaceutical preparations cannot be commercialized without strictly investigating detrimental effect to human, resulting in the environmental pollution that was caused by the leakage of toxic substance from scrapped industrial products. We the manufacturers must be responsible for characterizing the potential environmental effects and biological toxicity of novel nanomaterial products for industrial laborers and consumers before products are widely

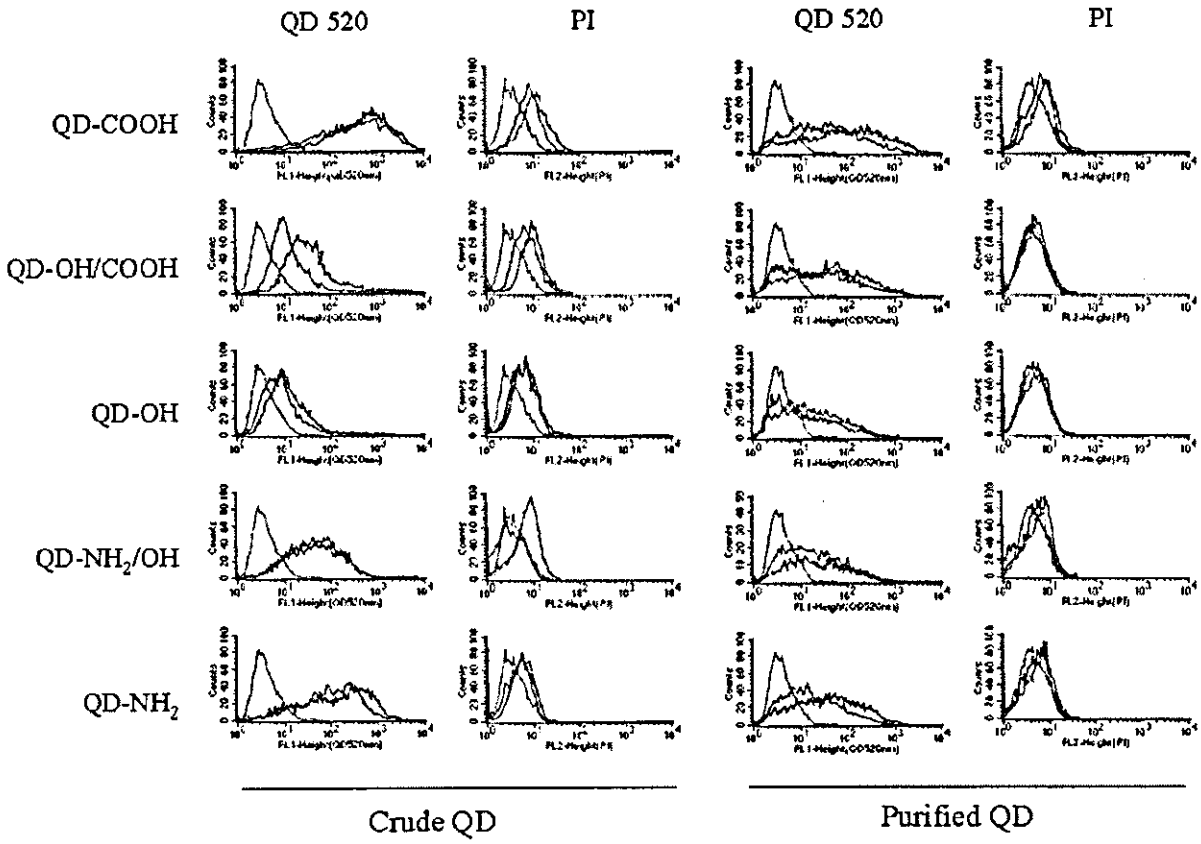

Figure 5. Contaminated impurities and ingredients in QD samples induce cell death. Vero cells were plated at 1×10^5 cells on 24-well plate and incubated for 12 h with crude QDs and ultrafiltration-purified QDs at 2 μM (red line) and 1 μM (blue line). Then cells were harvested, stained with propidium iodide, and analyzed by flow cytometry. The x axis indicates the fluorescence intensity of QDs (left columns) and PI (right columns) on a log scale. The green line shows untreated cells as a negative control. Results are representative of three separate experiments.

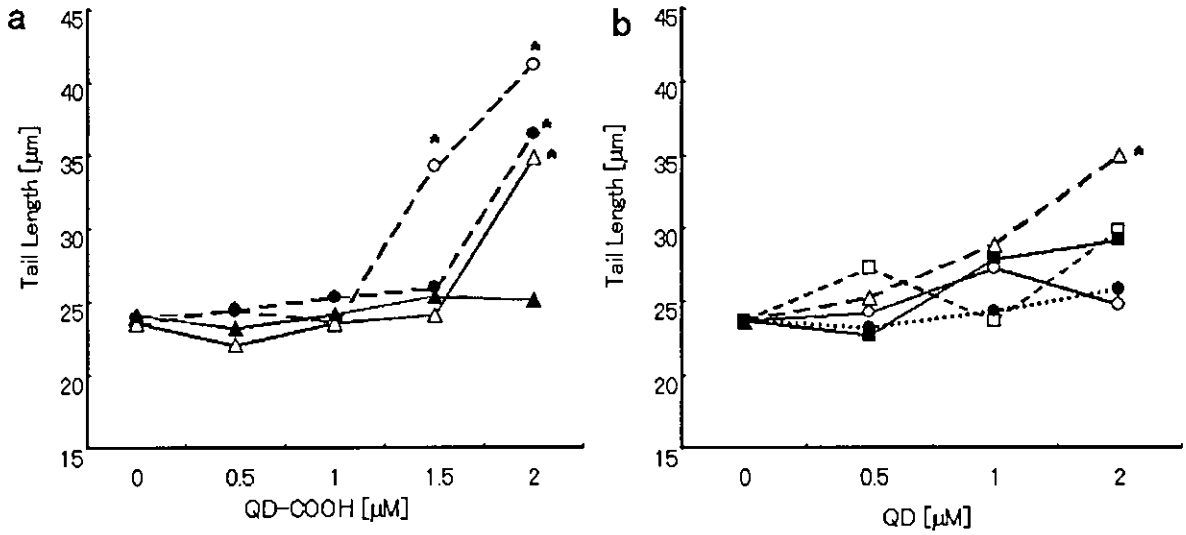

Figure 6. DNA-damaging effects of hydrophilic nanocrystalline QDs by comet assay. (a) WTK-1 cells were treated with QD-COOH (ultrafiltration purified; ▲, △) or QD-COOH (crude; ●, ○) for 2 h (open symbols) and 12 h (filled symbols). Then cells were harvested and embedded in 1% agarose, and electrophoresis was performed at 0 °C for 20 min at 25 V (0.96 V/cm) and approximately 250 mA. After being stained with ethidium bromide, the length of the whole comet was measured for 50 nuclei for each dose using a fluorescence microscope (200× magnification). (b) Cells were treated with QD-COOH (△), QD-NH_2 (□), QD-OH (○), QD-OH/COOH (●), or QD-NH_2/OH (■) for 2 h. The difference between the means in the treated and control plates was compared with the Dunnett test after one-way ANOVA. *, $p < 0.05$.

commercialized. In this paper, we revealed that the toxicity of QDs in biological systems is not dependent on the nanocrystal particle itself but on the surface molecules. In the case of QDs, no cytotoxicity was detected from their ingredients or the QD core itself, suggesting that surface processing will overcome the toxicity of nanomaterials. Less cytotoxicity derived from their ingredients or the QD core itself was observed in QD-OH in vitro. It is expected that QDs will be applied in the biomedical field for the innovative investigation, diagnosis, and medical treatment of various diseases.[9-12] When producing nanometer-sized materials in the future, it will be vital that the behavior of QDs in the biological system is not dependent on the chemical properties of surface-covered molecules but on the nanocrystalline particle itself. Surface modifications of functional molecules combined with nanoparticles may work as bionanomachines conforming to the functions designated by their surface molecules.

We conclude that the surface treatment of nanocrystals (surface-covered functional groups and biomolecules covering the surface of QDs) has specified the biological behavior of whole nanocrystalline QDs. We hope that the surface modifications of functional molecules combined with nanoparticles may work as a bionanomachine conforming to the functions designated by their surface molecules.

Acknowledgment. We are grateful to Dr. Akira Yuo and Dr. Taeko Dohi (Research Institute, IMCJ) for generously providing valuable advice about data collection. We thank Dr. Yukio Yamaguchi and colleagues (Department of Chemical System Engineering, University of Tokyo) for amino-QD improvements. This work was supported by a Medical Techniques Promotion Research Grant from the Ministry of Health, Labor and Welfare of Japan (H14-nano-004).

Supporting Information Available: Experimental procedures: Preparation of CdSe/ZnS fluorescent nanocrystal Qdots, preparation of surface-modified nanocrystal QDs, and protocols for comet assay and cell viability assays. This material is available free of charge via the Internet at http://pubs.acs.org.

References

(1) Colvin, V. L. *Nat. Biotechnol.* **2003**, *21*, 1166−1170.
(2) Borm, P. J. *Inhalation Toxicol.* **2002**, *14*, 311−324.
(3) Albrecht, C.; Borm, P. J.; Adolf, B.; Timblin, C. R.; Mossman, B. T. *Toxicol. Appl. Pharmacol.* **2002**, *184*, 37−45.
(4) Schins, R. P.; Duffin, R.; Hohr, D.; Knaapen, A. M.; Shi, T.; Weishaupt, C.; Stone, V.; Donaldson, K.; Borm, P. J. *Chem. Res. Toxicol.* **2002**, *15*, 1166−1173.
(5) Rosenthal, S. J.; Tomlinson, I.; Adkins, E. M.; Schroeter, S.; Adams, S.; Swafford, L.; McBride, J.; Wang, Y.; DeFelice, L. J.; Blakely, R. D. *J. Am. Chem. Soc.* **2002**, *124*, 4586−4594.
(6) Dubertret, B.; Skourides, P.; Norris, D. J.; Noireaux, V.; Brivanlou, A. H.; Libchaber, A. *Science* **2002**, *298*, 1759−1762.
(7) Jaiswal, J. K.; Mattoussi, H.; Mauro, J. M.; Simon, S. M. *Nat. Biotechnol.* **2003**, *21*, 47−51.
(8) Xu, H.; Sha, M. Y.; Wong, E. Y.; Uphoff, J.; Xu, Y.; Treadway, J. A.; Truong, A.; O'Brien, E.; Asquith, S.; Stubbins, M.; Spurr, N. K.; Lai, E. H.; Mahoney, W. *Nucleic Acids Res.* **2003**, *31*, 43.
(9) Wu, X.; Liu, H.; Liu, J.; Haley, K. N.; Treadway, J. A.; Larson, J. P.; Ge, N.; Peale, F.; Bruchez, M. P. *Nat. Biotechnol.* **2003**, *21*, 41−46.
(10) Chan, W. C.; Maxwell, D. J.; Gao, X.; Bailey, R. E.; Han, M.; Nie, S. *Curr. Opin. Biotechnol.* **2002**, *13*, 40−46.
(11) Zhu, L.; Ang, S.; Liu, W. T. *Appl. Environ. Microbiol.* **2004**, *70*, 597−598.
(12) Mattoussi, H.; Mauro, J. M.; Goldman, E. R.; Anderson, G. P.; Sundar, V. C.; Mikulec F. V.; Bawendi, M. G. *J. Am. Chem. Soc.* **2000**, *122*, 12142−12150.
(13) Gerion, D.; Pinaud, F.; Williams, S. C.; Parak, W. J.; Zanchet, D.; Weiss, S.; Alivisatos, A. P. *J. Phys. Chem. B* **2001**, *105*, 8861−8871.
(14) Hanaki, K.; Momo, A.; Oku, T.; Komoto, T.; Maenosono, S.; Yamaguchi, Y.; Yamamoto, K. *Biochem. Biophys. Res. Commun.* **2003**, *302*, 496−501.
(15) Medintz, I. L.; Clapp, A. R.; Mattoussi, H.; Goldman, E. R.; Fisher, B.; Mauro, J. M. *Nat. Mater.* **2003**, *9*, 630−638.
(16) Chan, W. C.; Nie, S. *Science* **1998**, *281*, 2016−2018.
(17) Goldman, E. R.; Balighian, E. D.; Mattoussi, H.; Kuno, M. K.; Mauro, J. M.; Tran, P. T.; Anderson, G. P. *J. Am. Chem. Soc.* **2002**, *124*, 6378−6382.
(18) Gao, X.; Chan, W. C.; Nie, S. *J. Biomed. Opt.* **2002**, *7*, 532−537.
(19) Akerman, M. E.; Chan, W. C.; Laakkonen, P.; Bhatia, S. N.; Ruoslahti, E. *Proc. Natl. Acad. Sci. U.S.A.* **2002**, *99*, 12617−12621.
(20) Larson, D. R.; Zipfel, W. R.; Williams, R. M.; Clark, S. W.; Bruchez, M. P.; Wise, F. W.; Webb, W. W. *Science* **2003**, *300*, 1434−1436.
(21) Mansson, A.; Sundberg, M.; Balaz, M.; Bunk, R.; Nicholls, I. A.; Omling, P.; Tagerud, S.; Montelius, L. *Biochem. Biophys. Res. Commun.* **2004**, *314*, 529−534.
(22) Pellegrino, T.; Parak, W. J.; Boudreau, R.; LeGros, M. A.; Gerion, D.; Alivisatos, A. P.; Larabell, C. A. *Differentiation* **2003**, *71*, 542−548.
(23) Levene, M. J.; Dombeck, D. A.; Kasischke, K. A.; Molloy, R. P.; Webb, W. W. *J. Neurophysiol.* **2004**, *91*, 1908−12.
(24) Dahan, M.; Levi, S.; Luccardini, C.; Rostaing, P.; Riveau, B.; Triller, A. *Science* **2003**, *302*, 442−445.
(25) Hoshino, A.; Hanaki, K.; Suzuki, K.; Yamamoto, K. *Biochem. Biophys. Res. Commun.* **2004**, *314*, 46−53.
(26) Singh, N. P.; McCoy, M. T.; Tice, R. R.; Schneider, E. L. *Exp. Cell. Res.* **1988**, *175*, 184−191.
(27) Sasaki, Y. F.; Tsuda, S.; Izumiyama, F.; Nishidate, E. *Mutat. Res.* **1997**, *388*, 33−44.
(28) Sasaki, Y. F.; Sekihashi, K.; Izumiyama, F.; Nishidate, E.; Saga, A.; Ishida, K.; Tsuda, S. *Crit. Rev. Toxicol.* **2000**, *30*, 629−799.
(29) Tice, R. R.; Agurell, E.; Anderson, D.; Burlinson, B.; Hartmann, A.; Kobayashi, H.; Miyamae, Y.; Rojas, E.; Ryu, J. C.; Sasaki, Y. F. *Environ. Mol. Mutagen.* **2000**, *35*, 206−221.
(30) Hines, M. A.; Guyot-Sionnest, P. *J. Phys. Chem.* **1996**, *100*, 468−471.
(31) Dabboussi, B. O.; Rodriguez-Viejo, J.; Mikulec, F. V.; Heine, J. R.; Mattoussi, H.; Ober, R.; Jensen, K. F.; Bawendi, M. G. *J. Phys. Chem. B* **1997**, *101*, 9463−9475.
(32) Reynolds, C. P.; Biedler, J. L.; Spengler, B. A.; Reynolds, D. A.; Ross, R. A.; Frenkel, E. P. *J. Natl Cancer Inst.* **1986**, *76*, 375−87.
(33) Liber, H. L.; Yandell, D. W.; Little, J. B. *Mutat. Res.* **1989**, *216*, 9−17.
(34) Bruchez, M., Jr.; Moronne, M.; Gin, P.; Weiss, S.; Alivisatos, A. P. *Science* **1998**, *281*, 2013−2016.

NL048715D

Microbiol. Immunol., 48(9), 669–675, 2004

Editor-Communicated Paper

On the Cyto-Toxicity Caused by Quantum Dots

Amane Shiohara[1,2], Akiyoshi Hoshino[1,2], Ken-ichi Hanaki[1], Kazuo Suzuki[2], and Kenji Yamamoto*[,1]

[1]*Department of Medical Ecology and Informatics, Research Institute, International Medical Center of Japan, Shinjuku-ku, Tokyo 162–8655, Japan, and* [2]*Department of Bioactive Molecules, National Institute of Infectious Diseases, Shinjuku-ku, Tokyo 162–8640, Japan*

Communicated by Dr. Hidechika Okada: Received June 21, 2004. Accepted June 29, 2004

Abstract: **Quantum dots (QDs) such as CdSe QDs have been introduced as new fluorophores. The QDs conjugated with antibody are starting to be widely used for immunostaining. However there is still not sufficient analysis of the toxicity of QDs in the literature. Therefore we evaluated the cell damage caused by the quantum dots for biological applications. We performed cell viability assay to determine the difference in cell damage depending on the sizes and colors of mercapto-undecanoic acid (MUA) QDs and the cell types. The results showed that the cell viability decreased with increasing concentration of MUA-QDs. But in the case of Vero cell (African green monkey's kidney cell) with red fluorescence QD (QD640), the cell damage was less than for the others. Furthermore through the flow cytometry assay we found that this cell damage caused by MUA-QD turned out to be cell death after 4–6-hr incubation. From the two assays described above, we found that there is a range of concentration of MUA-QDs where the cell viability decreased without cell death occurring and thus we conclude that attention should be given when MUA-QDs are applied to living organisms even in low concentrations.**

Key words: **Cell damage, MUA-QD, Cell death**

Quantum dots (QDs) such as CdSe QDs are nano-sized metal clusters. QDs have specific characteristics such as the quantum effect, which is a special photo quality caused by the widening of the band gap when the spatial dimension is reduced. Kubo et al. predicted the specific character of the quantum dot theoretically in 1962 (14–16). Since then, research concerning the applications of QDs has gained a great amount of interest. For example, in the field of Information Technology and optical-engineering (3, 10, 21, 29, 30), QDs have been proposed for use as a new material for memory, and as miniature laser-beam emitting devices. Furthermore, the biological applications of QDs conjugated with antibody have started to attract much attention, especially in immunostaining, separating cells, and diagnostics, because of their advantages such as longer lifetime and higher fluorescence over conventional organic fluorophores (1, 2, 8, 27). The first synthesized QDs are insoluble in biological solvents because non-polar groups of organic molecules are exposed on the surface of QDs. However the water-soluble QDs covered with mercapto-undecanoic acid (MUA) have been reported (2). In addition, the MUA-QD covered with sheep serum albumin (SSA) is well dispersed in water (2, 9). The advantages of MUA-QDs described above make it possible to consider the application of MUA-QDs to drug delivery systems (6, 20, 25, 28) as a drug-carrier and cell delivery system. Quantum dots have a longer lifetime compared to conventional organic fluorophores and thus make it easier to trace the drug delivered in living organisms. To make sure the application is feasible, an in-depth evaluation using MUA-QD in living organisms is needed. In fact cadmium (13) and selenium (24) are known to be toxic. Though the use of MUA-QDs for organisms has been known and some other studies about the actual injections into organisms have been conducted, the toxicity of MUA-QDs has not been reported in detail yet. Published works regarding

**Address correspondence to* Dr. Kenji Yamamoto, Department of Medical Ecology and Informatics, Research Institute, International Medical Center of Japan, 1-21-1, Toyama, Shinjuku-ku, Tokyo 162–8655, Japan. Fax: +81-3-3202-7364. E-mail: backen@ri.imcj.go.jp

Abbreviations: DMEM, Dulbecco's Modified Eagle's Medium; FCS, fetal calf serum; HC, human primary hepatocyte; MUA-QD, mercapto-undecanoic acid quantum dot; PBS, phosphate-buffered saline; PI, propidium iodide; SSA, sheep serum albumin; TOPO, tri-*n*-octylphosphine oxide.

QDs have so far only effectively assumed that QDs are safe. In this paper, we proceeded one step further by investigating the cell damage caused by MUA-QDs through an extensive and comprehensive experiment. We chose CdSe QDs because they are one of the QDs that have the strongest emission and they are used the most in many fields. In order to analyze the cell damage caused by MUA-QDs, a cell viability assay, which assesses the mechanism of glycolytic pathways, was conducted (12, 17, 26). Then in order to figure out whether the cell damage was cell death or not, we examined cell death using the flow cytometry assay.

Materials and Methods

Preparation of MUA-QDs. CdSe/ZnS QDs were synthesized in tri-*n*-octylphosphine oxide (TOPO) in accordance with the standard method (5, 11, 18, 19). For these experiments, three MUA-QDs were prepared; QD520, QD570 and QD640 which emitted green, yellow, and red, respectively.

Preparation of MUA-QDs solution with sheep serum albumin. The same volumes of 10 mg/ml MUA-QD and 10 mg/ml sheep serum albumin (SSA) were mixed as described in Hanaki et al. (9). Then we centrifuged this solution with a 0.45 μm filter at 5,000×*g* for 5 min at room temperature. The MUA-QD/SSA solution for all the cells was diluted with DMEM into several concentrations.

Cell viability assay. The cell viability was measured after the exposure of cells with MUA-QD to 2-(2-methoxy-4-nitrophenyl)-3-(4-nitrophenyl)-5-(2,4-disulfophenyl)-2H-tetrazolium, monosodium salt to generate hormazan. The number of the living cells is known to be proportional to the concentration of the generated hormazan (12, 26). Cell viability was measured for the following two cell lines and a primary cell culture; Vero cells (African green monkey kidney cells), HeLa cells, and human primary hepatocyte (HC). The above-mentioned cell types were cultured at 37 C, in 5% CO_2 in DMEM, supplemented with 5% heat-inactivated fetal calf serum (FCS). All the cells were suspended in DMEM, supplemented with 5% FCS and 50 μg/ml gentamicin after they had been treated with trypsin and centrifuged at 1,800 rpm for 5 min at room temperature. The cell count was performed for the three types of cells respectively. Each cell was plated into a 96-well plate (Iwaki Co., Tokyo) at 3×10^4 cells/well (100 μl/well). After a 24-hr incubation, the DMEM was removed and the prepared MUA-QD/SSA solution diluted to several different concentrations was poured into the wells. After another 24-hr incubation period, a Cell Counting Kit8 (Dojindo Laboratories Co., Kumamoto, Japan) was added into the 110 μl/well. The Cell Counting Kit8 was diluted with DMEM (Cell Counting Kit8:DMEM=1:10). Then the absorbances were measured at 450 nm by an absorptiometer (Molecular Devices Co.).

Flow cytometry assay. For the flow cytometry assay (23), in all the experiments, each cell was plated into a 12-well plate (Iwaki Co., Tokyo) at 10^6 cells/well (1,000 μl/well).

The cells were incubated for 24 hr. The culture medium was removed, and then the prepared MUA-QD/SSA solution diluted to several different concentrations was poured into the wells. After incubation, the cells were washed with PBS and the dead cells were stained with propidium iodide (PI) (4, 7) (0.1 mg/ml) for 5 min at room temperature, followed by treatment with Puck's EDTA solution (4 mM, $NaHCO_3$; 136 mM, NaCl; 4 mM, KCl; 1 mM, EDTA; 1 mg/ml, glucose), which will do less damage to cells than trypsin. The cells were suspended in PBS after they were fixed with 3% formaldehyde. Then, the fluorescence intensity of PI and QD520 was measured using the flow cytometry (Cyto Ace 300 JASCO, Tokyo) assay.

Results and Discussion

Cell Viability Assay

We conducted the cell viability assay to confirm whether the MUA-QDs do damage to the cells or not (12, 26). We used three cell types; Vero cell, HeLa cell, and primary human hepatocyte for three MUA-QDs (QD520, QD570, and QD640). Their spectrums are shown in Fig. 1. The result showed that MUA-QDs affect the cell viability even in rather low concentrations (Fig. 2). The tendencies of the cell viability with QD570 and QD520 were almost the same. However only in the case of QD640 with Vero cells does the result show a difference in cell viability of less than 0.4 mg/ml. The cell damage was less than for the others only in this experiment though the tendency was the same.

Flow Cytometry Assay

Cell viability assay is easy to handle and quantitatively good as well. However, if the intracellular activity is affected; for example, that of NADH-Dehydrogenase, the results will not reflect the true number of cells. Therefore fluorescence intensity of PI was measured using flow cytometry; another method of counting living cells based on a different principle. Figure 3 shows the result of the experiment incubated for 24 hr with QD520 (23).

Collins et al. reported that living cells do not take in

propidium iodide (PI), which has 610 nm fluorescent (4). Only QD520 was used for the flow cytometry assay because the emission peaks of QD570 and QD640 could not be distinguished from that of PI. The top two Figs. (without MUA-QD) show that the emission intensity obtained with a PI filter and that obtained with a QD filter were both quite low. The emission intensity obtained from the PI filter, however, increased gradually, according to the concentration of the MUA-QDs. At more than 0.15 mg/ml concentration of MUA-QDs, the emission intensity of PI was split into two peaks; the left peak shows the living cells, and the right peak shows the dead cells. On the other hand, in the right lane (with the QD filter), in the cases where the concentration of MUA-QD was more than 0.15 mg/ml, the emission intensity of MUA-QD increased, depending on the concentration of MUA-QDs. The higher emission peak contains both the damaged cells and the undamaged cells in the left panel. At the same time, however, the intensity of PI also increased steadily, which means that the population of dead cells increased from 0.15 mg/ml upward. The results showed the cell damage caused by MUA-QD is cell death.

To analyze the dependence on the incubation time, we measured the ratio of the damaged cells (PI stained cells) against the total number of the cells chronologically (Fig. 4). The ratio of damaged cells increased sharply from 4-hr incubation in 0.2 mg/ml concentration of MUA-QD, and slowly in 0.1 mg/ml. On the other hand, we cannot observe any difference between the result obtained from the concentration of 0.05 mg/ml and that from the control. The result from the flow cytometry assay is compatible with that from the cell viability assay in the view of the concentration of MUA-QD causing cell damage. Cell damage caused by MUA-QD probably occurs because the connection of SSA that covers MUA-QD is not a chemical bond; it just attaches to the surface of the MUA-QD (9). Therefore SSA is easy to remove from the surface of MUA-QD and MUA comes out to the surface. To solve this problem, the surface-processing should be reexamined. Safer materials should be used to coat the surface of QDs or new safer QDs, such as silicon-QD, etc., can be considered for use for the DDS. As for its application for the DDS, the coating with peptide is effective because the tagging of target-molecules will be necessary: Peptide is more easily applicable for pharmaceutical biology and it is much safer. What is more, we have seen the difference in the extent of the cell damage only in the case of the combination of Vero cells and

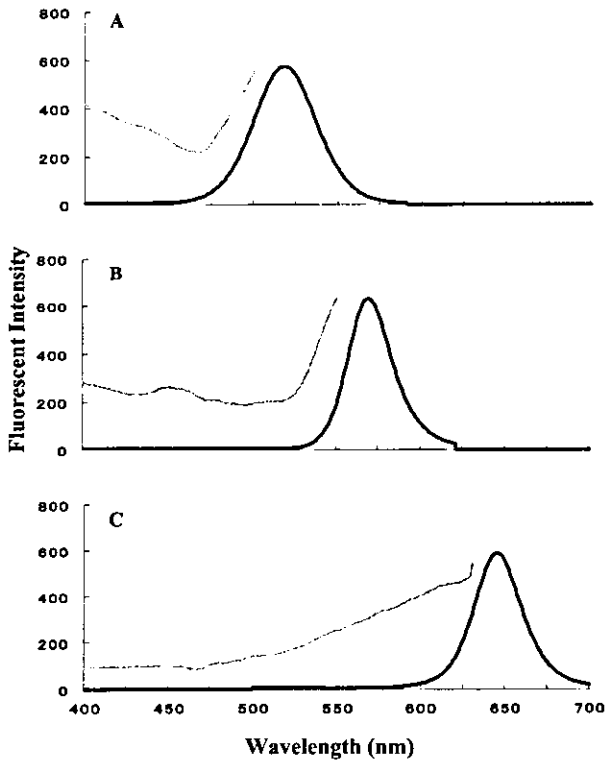

Fig. 1. Photoluminescent properties of three different MUA-QDs. (A) QD520, (B) QD570, and (C) QD640. Three different MUA-QDs were dissolved in DW, and their photoluminescent properties were measured with FP-6500. Emission spectra of QD520 excited at 300 nm, QD570 excited at 350 nm, and QD640 excited at 360 nm, represented as black lines. Excitation spectra represented as gray lines collected with detection at the respective peak spectra.

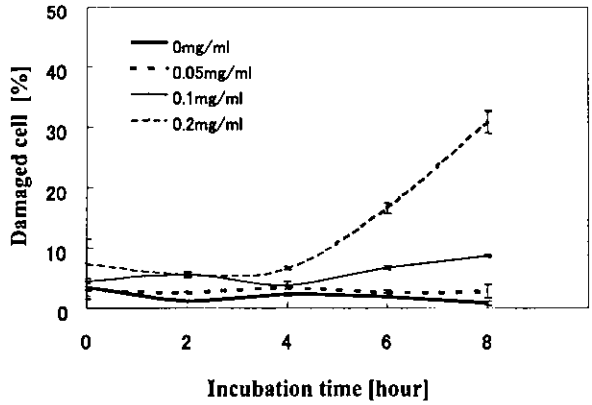

Fig. 4. Flow cytometry assay for the effect of the incubation time difference and concentration of QD. Vero cell and QD520 were used for this experiment. The vertical axis stands for the damaged cell % (the ratio of the number of the PI stained cell against the total number of cells). The intensity of PI is measured between 565 and 605 nm, and the intensity of QD520 is measured between 515 and 545 nm. The horizontal axis stands for the incubation time of the cell. The bold line stands for a concentration of QD520 at 0 mg/ml, the broken line stands for a concentration of 0.05 mg/ml, the solid line, 0.1 mg/ml, and the dotted line, 0.2 mg/ml. The vertical lines are the error bars.

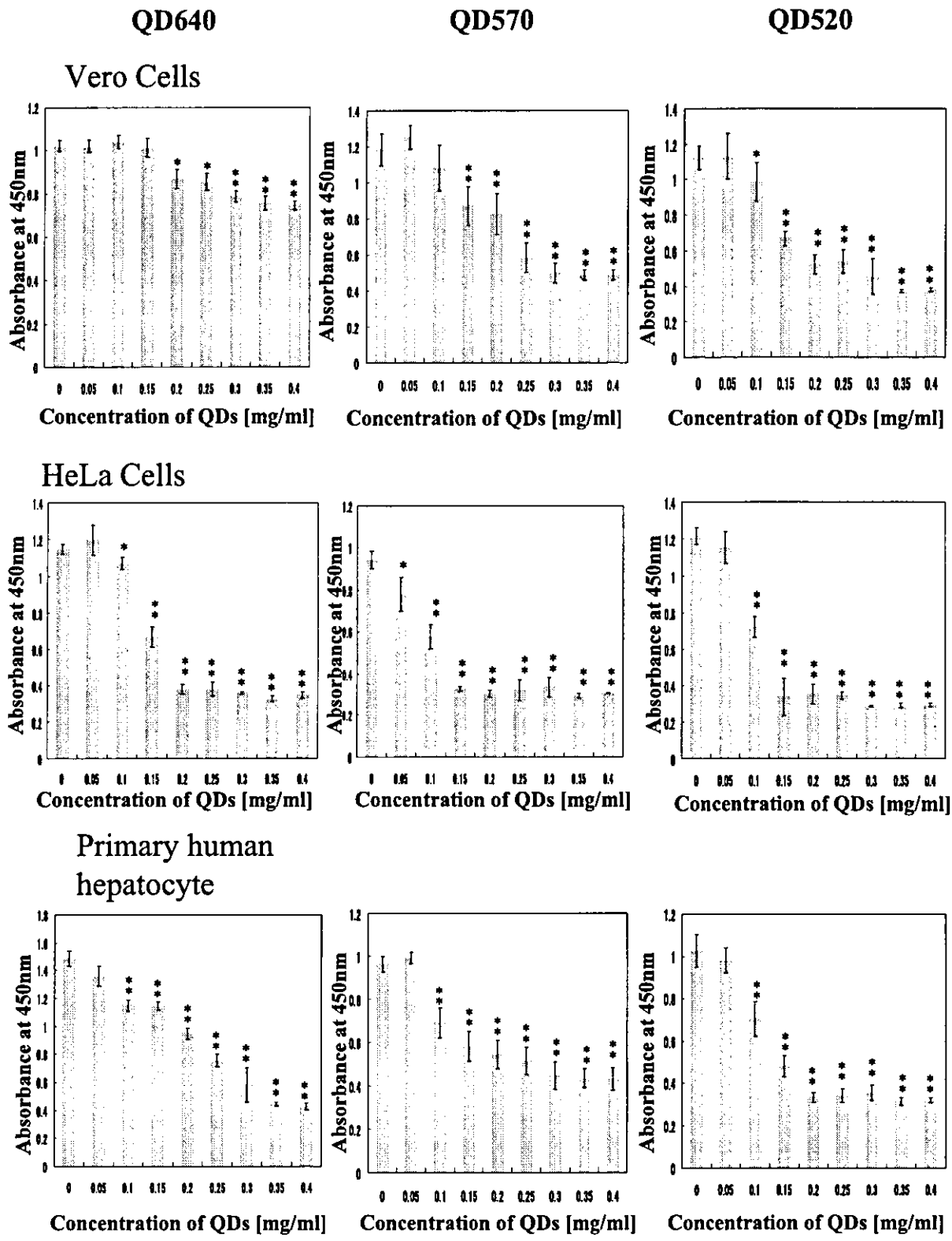

Fig. 2. Cell viability for the different sizes of the QDs and different cell types. Three of the different sizes of QDs are tested on the cell viability for each cell type (MTT assay, $n=5$). The top three panels stand for the cell viabilities of Vero cells, those in the middle for HeLa cells, and those in the bottom for primary human hepatocyte. The three panels in the left lane stand for QD640, those in the middle lane for QD570, and those in the right lane for QD520. In each panel, the horizontal axis stands for the concentration of QD, and the vertical axis stands for the absorbance at 450 nm. The columns in all the panels stand for the amount of hormazan, which reflect the cell viability, and I is standard deviation. A T-test was performed; * stands for the significance level <0.01, and ** stands for the significance level <0.001.

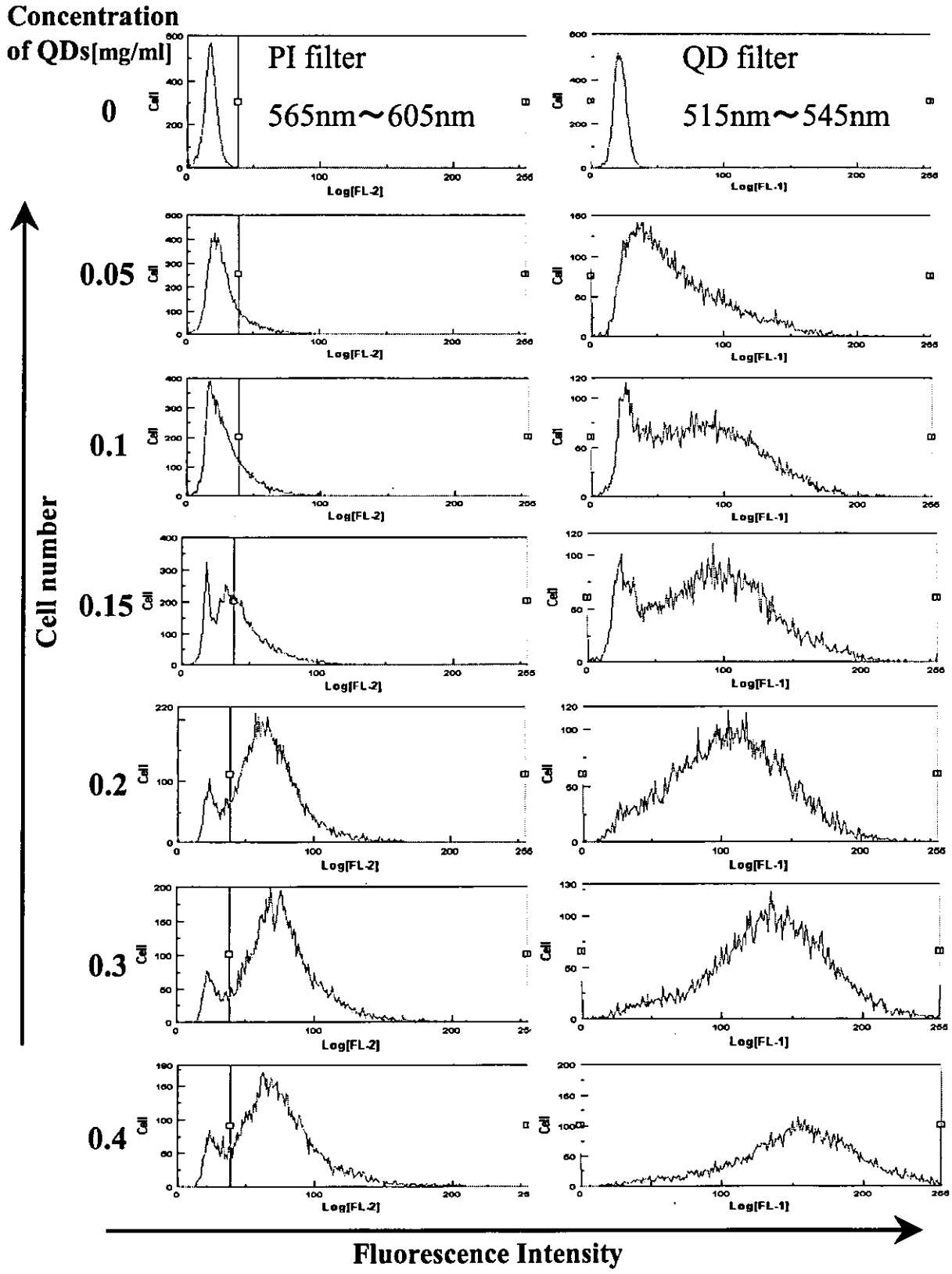

Fig. 3. Flow cytometry assay with the different concentrations of QD. Vero cell and QD520 are used for the flow cytometry assay. The horizontal axis, in the left lane, is the fluorescent intensity of propidium iodide with the filter (565 nm–605 nm), and in the right lane, the fluorescent intensity of QD520 with the filter (515 nm–545 nm). The vertical axes, in both the columns, stand for the cell count. Each row, from the top to the bottom, is given with respect to the concentration of QD520. In each row, the left panel and the right panel show the result with the same sample measured with a PI filter (left) and a QD filter (right), respectively.

QD640. It has been strongly suggested that the mobility of the MUA-QDs inside the cell depends on the size of the MUA-QDs (22). This might also explain the difference in the cell damage in our study.

In order to utilize quantum dots for humans, further study should be done on the relationship between the cell type and MUA-QD cell damage, an estimate of the mutation rate in bacteria and carcinogenesis in animals should be done and research into the mechanism of cyto-toxicity is needed. So far there is currently insufficient information about the discharge of MUA-QDs from living organisms.

We are grateful to Dr. Ohta of Tokyo University of Pharmacy and Life Science for his help with data collection, and proofreading. This work was supported by Grant 'H14-nano-004' of the Ministry of Health, Labour and Welfare of Japan.

References

1) Bruchez, M., Jr., Moronne, M., Gin, P., Weiss, S., and Alivisatos, A.P. 1998. Semiconductor nanocrystals as fluorescent biological labels. Science **281**: 2013–2016.
2) Chan, W.C., and Nie, S. 1998. Quantum dot bioconjugates for ultrasensitive nonisotopic detection. Science **281**: 2016–2018.
3) Coe, S., Woo, W.K., Bawendi, M., and Bulovic, V. 2002. Electroluminescence from single monolayers in molecular organic devices. Nature **420**: 800–803.
4) Collins, A.M., and Donoghue, A.M. 1999. Viability assessment of honey bee, Apis mellifera, sperm using dual fluorescent staining. Theriogenology **51**: 1513–1523.
5) Dabbousi, B.O., Rodriguez-Viejo, J., Mikulec, F.V., Heine, J.R., Mattoussi, H., Ober, R., Jensen, K.F., and Bawendi, M.G. 1997. (CdSe) ZnS core-shell quantum dots: synthesis and characterization of a size series of highly luminescent nanocrystallites. J. Phys. Chem. B **101**: 9463–9475.
6) Dubertret, B., Skourides, D., Norris, J., Noireaux, V., Brivanlou, A.H., and Libchaber, A. 2002. *In vivo* imaging of quantum dots encapsulated in phospholipid micelles. Science **298**: 1759–1762.
7) Elstein, K.H., and Zucker, R.M. 1994. Comparison of cellular and nuclear flow cytometric techniques for discriminating apoptotic subpopulations. J. Neurochem. **74**: 1041–1048.
8) Gerion, D., Pinaud, F., Williams, S.C., Parak, W.J., Zanchet, D., Weiss, S., and Alivisatos, A.P. 2001. Synthesis and properties of biocompatible water-soluble silica-coated CdSe/ZnS semiconductor quantum dots. J. Phys. Chem. B **105**: 8861–8871.
9) Hanaki, K., Momo, A., Oku, T., Komoto, A., Maenosono, S., Yamaguchi, Y., and Yamamoto, K. 2003. Semiconductor quantum dot/albumin complex is a long-life and highly photostable endosome marker. Biochem. Biophys. Res. Commun. **302**: 496–501.
10) Harman, T.C., Taylor, P.J., Walsh, M.P., and LaForge, B.E. 2002. Quantum dot superlattice thermoelectric materials and devices. Science **297**: 2229–2232.
11) Hines, M.A., and Guyot-Sionnest, P. 1996. Synthesis and characterization of strongly luminescing ZnS-capped CdSe nanocrystals. J. Phys. Chem. **100**: 468–471.
12) Ishiyama, M., Miyazono, Y., Sasamoto, K., Ohkura, Y., and Ueno, K. 1997. A highly water-soluble disulfonated tetrazolium salt as achromogenic indicator for NADH as well as cell viability. Talanta **44**: 1299.
13) Kondoh, M., Araragi, S., Sato, K., Higashimoto, M., Takiguchi, M., and Sato, M. 2002. Cadmium induces apoptosis partly via caspase-9 activation in HL-60 cells. Toxicology **170**: 111–117.
14) Kubo, R. 1957. Statistical-mechanical theory of irreversible processes. I. J. Phys. Soc. Jpn. **12**: 570–586.
15) Kubo, R. 1962. Generalized cumulant expansion method. J. Phys. Soc. Jpn. **17**: 1100–1120.
16) Kubo, R. 1962. Stochastic liouville equations. J. Math. Phys. **4**: 174–183.
17) Mosman, T. 1983. Rapid colorimetric assay for cellular growth and survival: application to proliferation and cytotoxicity assays. J. Immunol. Methods **65**: 55–63.
18) Murray, C.B., Norris, D.J., and Bawendi, M.G. 1993. Synthesis and characterization of nearly monodisperse CdE (E=sulfur, selenium, tellurium) semiconductor nanocrystallities. J. Am. Chem. Soc. **155**: 8706–8715.
19) Peng, X., Schlamp, M.C., Kadavanich, A.V., and Alivisatos, A.P. 1997. Epitaxial growth of highly luminescent CdSe/CdS core/shell nanocrystals with photostability and electronic accessibility. J. Am. Chem. Soc. **119**: 7019–7029.
20) Rosenthal, S.J., Tomlison, I., Adkins, E.M., Schroeter, S., Adams, S., Swafford, L., McBride, J., Wang, Y., Defelice, L.J., and Blakely, R.D. 2002. Targeting cell surface receptors with ligand-conjugated nanocrystals. J. Am. Chem. Soc. **124**: 4586–4594.
21) Santori, C., Fattal, D., Vuckovic, J., Solomon, G.S., and Yamamoto, Y. 2002. Indistinguishable photons from a single-photon device. Nature **419**: 594–597.
22) Seydel, C. 2003. Quantum dots get wet. Science **300**: 80–81.
23) Shatrova, A.N., Aksenov, N.D., Poletaev, A.I., and Zenin, V.V. 2003. Effect of etoposide and amsacrine on mitotic progression of GM-130 and Hep-2 cell lines. The flow cytometry assay. Tsitologiia **45**: 59–68.
24) Shen, H.M., Yang, C.F., and Ong, C.N. 1999. Sodium selenite-induced oxidative stress and apoptosis in human hepatoma HepG2 cells. Int. J. Cancer **81**: 820–828.
25) Shubeita, G.T., Sekatskii, S.K., Dietler, G., Potapova, I., Mews, A., and Basch, T. 2003. Scanning near-field optical microscopy using semiconductor nanocrystals as a local fluorescence and fluorescence resonance energy transfer source. J. Microsc. **210**: 274–278.
26) Tominaga, H., Ishiyama, M., Ohseto, F., Sasamoto, K., Hamamoto, T., Suzuki, K., and Watanabe, M. 1999. A water-soluble tetrazolium salt useful for colorimetric cell viability assay. Anal. Commun. **36**: 47.
27) Wu, X., Liu, H., Liu, J., Haley, K.N., Treadway, J.A., Larson, J.P., Ge, N., Peale, F., and Bruchez, M.P. 2002. Immunofluorescent labeling of cancer marker Her2 and other cellular targets with semiconductor quantum dots.

Nat. Biotechnol. **21**: 41–46.

28) Xu, H., Sha, M.Y., Wong, E.Y., Uphoff, J., Xu, Y., Treadway, J.A., Truong, A., O'Brien, E., Asquith, S., Stubbins, M., Spurr, N.K., Lai, E.H., and Mahoney, W. 2003. Multiplexed SNP genotyping using the Qbead system: a quantum dot-encoded microsphere-based assay. Nucleic Acids Res. **31**: 43.

29) Wu, L.X., Steel, D.Y., Gammon, D., Stievater, T.H., Katzer, D.S., Park, D., Piermarocchi, C., and Sham, L.J. 2003. An all-optical quantum gate in a semiconductor quantum dot. Science **301**: 809–811.

30) Zrenner, A., Beham, E., Stufler, S., Findeis, F., Bichler, M., and Abstreiter, G. 2002. Coherent properties of a two-level system based on a quantum-dot photodiode. Nature **418**: 612–614.

Microbiol. Immunol., 48(12), 985–994, 2004

Editor-Communicated Paper

Quantum Dots Targeted to the Assigned Organelle in Living Cells

Akiyoshi Hoshino[1,2,3], Kouki Fujioka[1], Taisuke Oku[1,4], Shun Nakamura[5], Masakazu Suga[1], Yukio Yamaguchi[4], Kazuo Suzuki[3], Masato Yasuhara[2], and Kenji Yamamoto*[,1,2]

[1]*Department of Medical Ecology and Informatics, Research Institute, International Medical Center of Japan, Shinjuku-ku, Tokyo 162–8655, Japan,* [2]*Department of Pharmacokinetics and Pharmacodynamics, Hospital Pharmacy, Tokyo Medical and Dental University, Bunkyo-ku, Tokyo 113–8519, Japan,* [3]*Department of Bioactive Molecules, National Institute of Infectious Diseases, Shinjuku-ku, Tokyo 162–8640, Japan,* [4]*Department of Chemical System Engineering, School of Engineering, University of Tokyo, Bunkyo-ku, Tokyo 113–8656, Japan, and* [5]*Division of Biochemistry and Cellular Biology, National Institute of Neuroscience, Kodaira, Tokyo 187–8502, Japan*

Communicated by Dr. Hidechika Okada: Received October 8, 2004. Accepted October 21, 2004

Abstract: **Fluorescent nanocrystal quantum dots (QDs) have the potential to be applied to bioimaging since QDs emit higher and far longer fluorescence than conventional organic probes. Here we show that QDs conjugated with signal peptide obey the order to transport the assigned organelle in living cells. We designed the supermolecule of luminescent QDs conjugated with nuclear- and mitochondria-targeting ligands. When QDs with nuclear-localizing signal peptides were added to the culture media, we can visualize the movements of the QDs being delivered into the nuclear compartment of the cells with 15 min incubation. In addition, mitochondrial signal peptide can also transport QDs to the mitochondria in living cells. In conclusion, these techniques have the possibility that QDs can reveal the transduction of proteins and peptides into specific subcellular compartments as a powerful tool for studying intracellular analysis *in vitro* and even *in vivo*.**

Key words: **Quantum dot, Signal peptide, Nanocrystal, Nuclear localizing signal, Mitochondria targeting signal, Bioimaging**

Nanotechnology is the technology of designing, manufacturing, and utilizing the "supermolecule materials" which have the specific function based on their nanometer size. The "supermolecule" said here is a functional unit of two meanings; (1) A supermolecule consists of each molecule that has a certain mutual interaction and relation with one another, (2) A supermolecule shows its specific function as a whole molecule. Ultrafine nanocrystals have been expected to be applied widely in biomedical fields as biomaterials, immunoassay, diagnostics, and even in therapeutics (7, 9, 18, 32, 34, 40, 41). One of them, nanocrystal quantum dots (QDs), is widely used as stable and bright fluorophores that can have high quantum yields, narrow luminescent spectra, high absorbency, high resistance to photobleaching, and can provide excitation of several different emission colors using a single wavelength for excitation (4, 19).

In the field of molecular biology, fluorescent tagging of cells and biomolecules with organic fluorophores such as FITC has been used for a long time for these purposes of tracking biomolecules. But unfortunately, the use of organic fluorophores for living-cell applications is subject to certain limitations, because most of fluorophores photobleach easily (17). These organic fluorophores have their broad emission bands, which limit the number of fluorescent probes that can be simultaneously resolved. In addition, there are a lot of bright fluorophores, such as Hoechst® dyes and a rhodamine 123 derivative (Mitotracker®) (20), used for stain of nuclei and mitochondria, but these fluorophores cannot transport proteins or other molecules to the target

**Address correspondence to* Dr. Kenji Yamamoto, Department of Medical Ecology and Informatics, Research Institute, International Medical Center of Japan, Toyama 1–21–1, Shinjuku-ku, Tokyo 162–8655, Japan. Fax: +81–3–3202–7364. E-mail: backen@ri.imcj.go.jp

Abbreviations: MPA, 3-mercaptopropanoic acid; QD, quantum dot; TOPO, *n*-trioctylphosphine oxide.

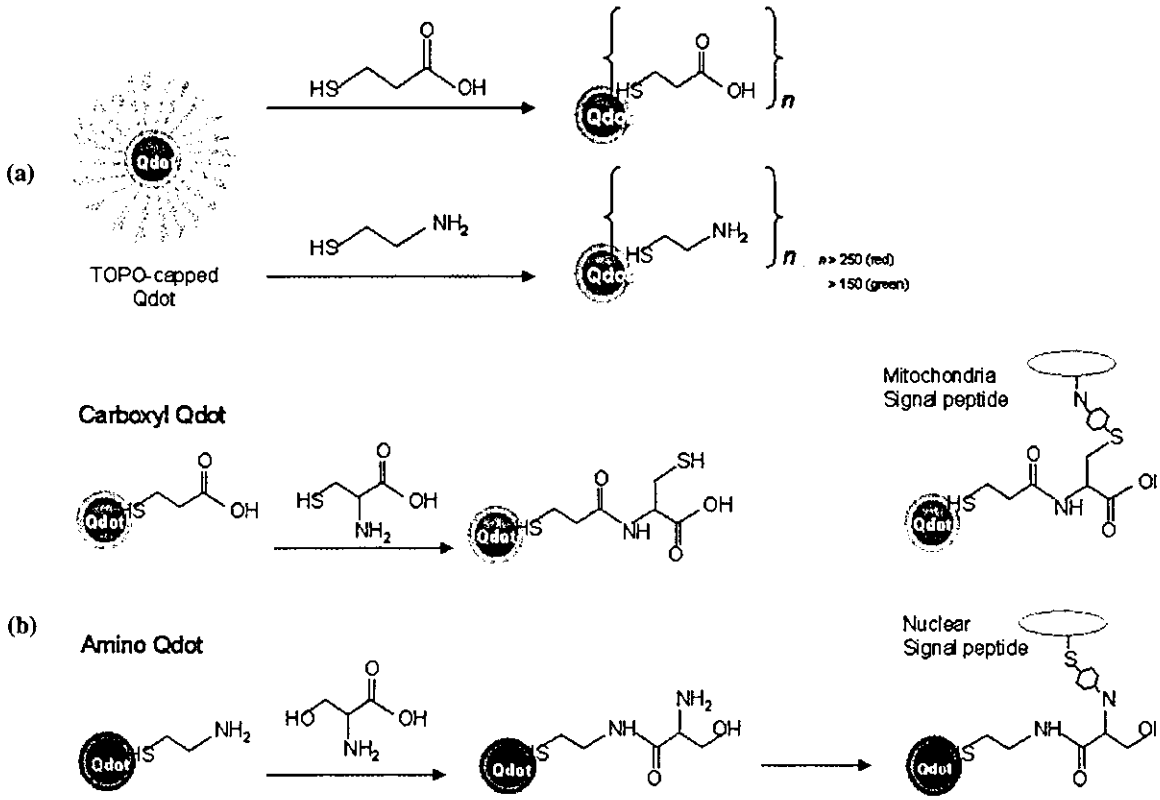

Fig. 1. Schematic illustration of peptide conjugated QDs for organelle targeting and imaging. (a) Chemically synthesized TOPO-capped QDs were replaced by MPA or cysteamine using thiol-exchange reactions. After reaction, QDs were covered with approximately 250 carboxyl or amine groups per particle. (b) A two-step conjugation strategy of QD-oligopeptide probes. MPA-QD (upper lane) or cysteamine-QD (lower lane) was primarily coupled with amine groups of cysteine or serine by using EDC coupling reagents. Then amino acid-coated QDs were secondarily conjugated with target peptides by coupling between *N*-hydroxysuccinimidyl and maleimide groups.

organelle. On the other hand, the signal peptides with organic fluorophore cannot trace the luminescent for long time observation. In contrast, QDs are stabilized over a far longer exposure-time to light and can emit fluorescence of higher luminosity than the conventional organic fluorescence probes (5, 8, 27). Therefore, QDs are suitable for designing the supermolecule that supplemented the biological effects to itself, and applications with QDs are now widely performed as long-time fluorescent markers for efficient collection of fluorescence (3, 17, 22, 24, 35).

Once our synthesized QDs were enfolded into the hydrophobic micelles and completely dissolved in aqueous solution, which promotes several innovations to improve the solubility to apply for biological methods (2, 10, 11, 23). The water-soluble QDs in our previous method have lower stability for low pH or salt-containing buffer (14). There is very little amount of conjugate by using these QDs, since the most of QDs were easily aggregated under the conditions that combine QD with peptides or protein. Therefore, we could only utilize QDs as the high fluorescence cell-tracking markers (14, 33). We previously reported that several novel surface-modified QDs using carboxylic acids, polyalcohols, or amines showed various physicochemical properties (16). In this article, we established a two-step conjugating method as shown in Fig. 1. The QDs of carboxyl groups were primarily coupled with amine groups of cysteine monomer, and QDs of amine groups were with carboxylic groups of serine monomer, respectively. The obtained amino acid-coated QDs, which were stable for the pH changes, were secondarily conjugated with target peptides/proteins by using their sulfhydryl and amine groups.

Some proteins and peptides have been demonstrated to penetrate through the plasma membrane of cells by their protein transduction domains (12, 21, 26, 31). Previous studies defined that protein transduction by nuclear localizing peptides was an efficient method to deliver proteins into the nuclei of cells (25, 37). In this study we tried to label two functional oligopeptides transported to nuclear localizing or mitochondria, and

evaluated whether QD-peptide complex worked as the specific functional supermolecule based on original peptides.

Materials and Methods

Synthesis of hydrophilic QDs. Synthesis of ZnS-coated CdSe nanocrystal QDs (fluorescence wavelength: approximately 642 nm emitted red, and approximately 518 nm emitted green), which were enfolded into the micelle of *n*-trioctylphosphine oxide (TOPO), was previously reported (6, 15). 3-Mercaptopropanoic acid (MPA) and 2-aminoethanethiol (cysteamine hydrochloride) were used to obtain two kinds of hydrophilic QDs (carboxyl- and amino-QDs) by thiol exchange methods. In the case of carboxyl-QD, 50 mg of TOPO-QDs were dissolved into 1 ml tetrahydrofuran (THF) in a 4 ml-volume flasket, and then 250 μl MPA (Sigma-Aldrich, St. Louis, Mo., U.S.A.) were added. Then the mixture was heated at 85 C for 24 hr. In the case of amino-QD, primarily 250 mg cysteamine (Wako Pure Chemicals, Tokyo) was heated at 85 C in a flask (16). After melting, 50 mg/ml TOPO-QDs in THF was dropped to the flask and heated at 85 C for 2 hr. After the reaction, the turbid solution was collected and centrifuged at maximum speed. After it dried up, purified water was added to the residue, and centrifuged at maximum speed to remove the insoluble residue. The supernatant fraction containing soluble QDs was collected. After purified by Sephadex G-25 column (Amersham Biosciences, Piscataway, N.J., U.S.A.), QDs were concentrated and powderized by vacuum distillation. QDs were reconstituted in purified water before use.

Preparation of peptide-conjugated QDs. Amino acid sequences of three well-known functional oligopeptides described below were chemically synthesized; nuclear localizing peptide ($R_{11}KC$, sequenced NH_2-RRRRRRRRRRRKC-COOH) (25), mitochondria targeting signal sequence of cytochrome-*c* oxidase VIII subunit (Mito-8, sequenced NH_2-MSVLTPLLLRGLTGSARRLPVPRAKIHWLC-COOH) (13) or control mitochondrial peptide (START, sequenced NH_2-STARTSTARTSTARTSC-COOH) (1). The peptides were conjugated to QDs by a two-step reaction. Initially, 100 μM QD solution was mixed with equal volume of 100 mM cysteine solution in coexistent with 100 mM EDC coupling reagents (Pierce Biotechnology, Rockford, Ill., U.S.A.) and continuously mixed at 4 C for 1 hr. After removed of free-amino acid by Nap-5 column (Amersham Biosciences), about 10-fold mol of target peptides were secondarily conjugated with QD by using sulfo-SMCC coupling reagents (Pierce Biotech) and sonicated for 2 hr at 4 C. Products were purified using ultra-filtration membrane (NMWL 10000, Centriprep® Millipore). Finally, purified QD-peptide conjugates were filtrated with 0.1-μm membrane filters (Millipore) before use. To analyze the protein content of QD-conjugated peptides, conjugated QDs was plated to 96-well microplate and RC-DC Protein Assay reagent (Bio-Rad, Hercules, Calif., U.S.A.) was added. Six hundred fifty nanometer absorbance was measured by microplate reader (Bio-Rad). MPA-coated QD without coupling with any peptides was used as negative control.

Assessment of QD-uptake by cells. Vero cells were cultured in DMEM/F12 supplemented with 5% heat-inactivated fetal bovine serum at 37 C. To avoid the non-specific binding of QDs on the glass, 10 mm glass-based culture dish (Matsunami Glass Industries, Japan) was pre-coated with poly-L-lysine (Peptide Institute Co., Ltd., Osaka, Japan). The cells were plated at a volume of 1×10^5 cells/well on a glass-based dish. Then cells were stimulated with the indicated concentration of QD-peptides. After incubation, the cells were washed with PBS 5 times to remove the non-specific binding QDs, and the cells were fixed, and embedded in the glycerol containing 0.1% sodium azide. In the case of co-localization assay, cells were observed with a confocal microscopy MRC-1024 (Bio-Rad). Time course of $R_{11}KC$-coated QDs was examined on the fluorescence microscopy system equipped with a CO_2 incubator (IM-310 cell-culture microscope system, Olympus, Japan). Images were acquired with a digital camera D1X (Nikon) under fluorescent microscopy IX-81 (Olympus) using WIR mirror unit to adjust excitation wavelength over 610 nm.

Results and Discussion

Some oligopeptides have been demonstrated to penetrate across the cellular membrane by their protein transduction domains and specifically located to their designated organelle (12, 21, 26, 31). Previous studies showed that the protein transduction by nuclear localizing signal oligopeptide was an efficient method of delivering proteins into the nuclei of cells (37). To establish the supermolecule design that supplemented the biological effects to nanocrystal, we conjugated two kinds of functional NLS and MTS oligopeptides, which were transported to nuclear or mitochondria (13, 25). Then we evaluated that QD-peptide complex worked as the specific supermolecule those functions were based on their original peptides.

For the achievements of assemble QD-supermolecule, we established a two-step conjugating method as shown in Fig. 1. Briefly, QDs were coupled with amino